3pPPb5

Auditory Engineering Laboratory

MODELING OF AUDITORY NERVE FIBER INPUT/OUTPUT FUNCTIONS NEAR THRESHOLD

Ian C. Bruce[1], Abigail Buller[2] and Muhammad S. A. Zilany[3]

[1]Department of Electrical & Computer Engineering, McMaster University, Hamilton, ON, Canada

[2]Department of Engineering Physics, McMaster University, Hamilton, ON, Canada

[3]Department of Electrical and Computer Engineering, Texas A&M University at Qatar, Doha, Qatar

McMaster University

ABSTRACT

The instantaneous discharge rate of auditory nerve fibers (ANFs) near their threshold exhibits an approximately exponential relationship to the instantaneous pressure at the eardrum after compensating for the delay latency. Some simplified models of the pressure-to-discharge transduction process in the cochlea have attributed this exponential relationship to an inner hair cell (IHC) transduction current that is either an exponential function with a level-dependent slope parameter or a first-order Boltzmann function (which is approximately exponential around the zero-input point) followed by a low-pass filter. However, such IHC transduction functions do not produce level-dependent changes in the AC and DC components of the IHC potential that match the behavior observed in physiological recordings.

In this study, we show that retaining the physiologically-accurate IHC transduction model of Bruce et al. (2018) and following it by an exponential or exponential-like function that maps the IHC potential to the input of the synaptic power-law adaptation in that model produces the desired exponential input/output behavior near threshold while preserving the appropriate level-dependent changes in ANF discharge rate and phase-locking.

I. INTRODUCTION

- Several detailed models have been developed of the mammalian auditory periphery that can explain a wide range of physiological data from auditory nerve fibers (ANFs) in response to a variety of acoustic stimuli (Osses Vecchi et al., 2022).
- One recent physiological observation by Horst et al. (2018) that has not been investigated with these detailed models is that ANF input/output (I/O) functions, i.e., the relationship between the instantaneous discharge rate and the instantaneous pressure at the eardrum after compensating for the mean discharge latency, is approximately exponential near a fiber's threshold (see Fig. 1).

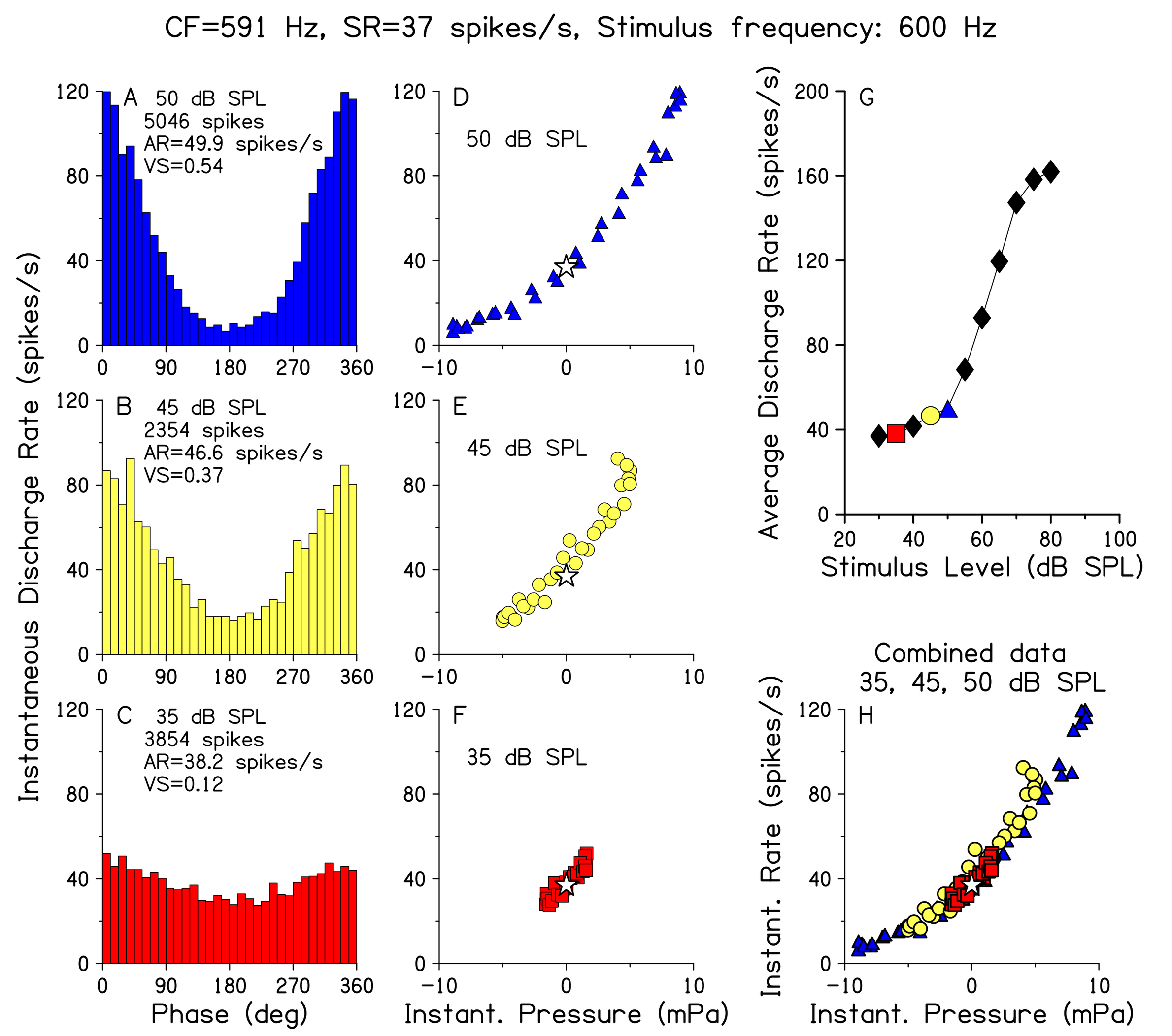

Figure 1: Example data for a low characteristic frequency (CF), high spontaneous rate (SR) cat ANF. A–C: Period histograms for three different sound pressure levels around this fiber's threshold. D–F: Corresponding I/O curves at those three presentation levels. G: Rate-level function for this fiber. H: Combined plot of the three I/O curves. Reprinted from Fig. 4 of Horst et al. (2018).

- Peterson and Heil (2020) proposed a simple phenomenological model, shown in Fig. 2, to explain cat ANF period histograms that included a Boltzmann function for inner hair cell (IHC) transduction followed by lowpass filtering to give the IHC potential and an exponential function mapping the IHC potential to synaptic drive to the ANF. Peterson and Heil (2021) demonstrated that their model also produces good fits to ANF rate-level curves.

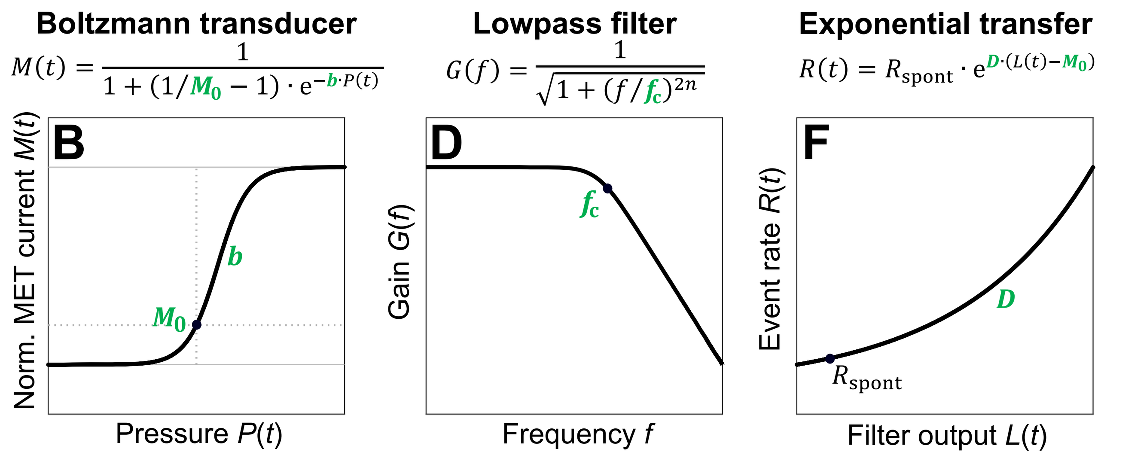

Figure 2: Phenomenological model proposed by Peterson & Heil of the transduction from a sound pressure waveform to synaptic drive (from an IHC to an ANF). Adapted from Fig. 1 of Peterson and Heil (2020).

- However, the Boltzmann IHC transduction function leads to hard saturation of the IHC potential, whereas physiological recordings from IHCs exhibit more gradual saturation (see Fig. 3A).
- In contrast, the IHC transduction function of Zhang et al. (2001) that has been retained in the subsequent versions of the Carney–Bruce–Zilany model captures this gradual saturation (see Fig. 3B).

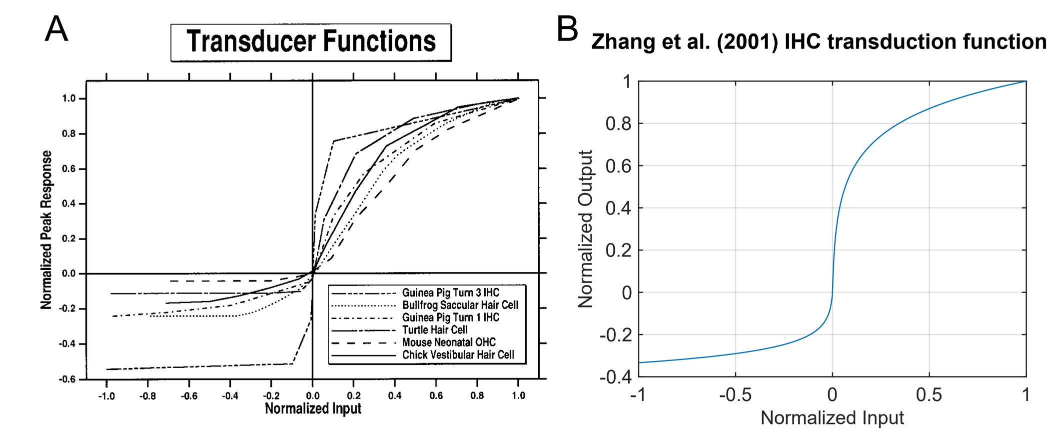

Figure 3: A: Transduction functions from a different types of hair cells, including IHCs, reprinted from Fig. 9 of Cheatham and Dallos (2000). B: Model IHC transduction function from Zhang et al. (2001) and subsequent models in that series.

- The behavior of the model fibers' I/O functions near threshold was not investigated by Zhang et al. (2001), but that model did include an exponential-like *softplus* function after IHC low-pass filtering, providing the mapping from the IHC potential to the input of the double-exponential adaptation stage of the model (Fig. 4A).
- The softplus function (Dugas et al., 2000), which has the form $\log_e[1 + e^x]$, is exponential for negative and small positive inputs and becomes linear for higher positive input values (Fig. 4D).
- The softplus function was retained in subsequent versions of the model (Fig. 4A) in which parallel power-law adaptation stages were added after the double-exponential adaptation (Zilany et al., 2014, 2009).
- Bruce et al. (2018) substantially changed the form of the double-exponential adaptation stage of the model and moved it to after the power-law adaptation. The mapping function from the IHC potential to the input of the power-law adaptation in that model is a very gradually saturating symmetrical nonlinearity with a slope parameter that varies as a function of characteristic frequency (CF) and desired spontaneous rate (SR), so we will refer to it as an "approximately linear" function (Fig. 4B).

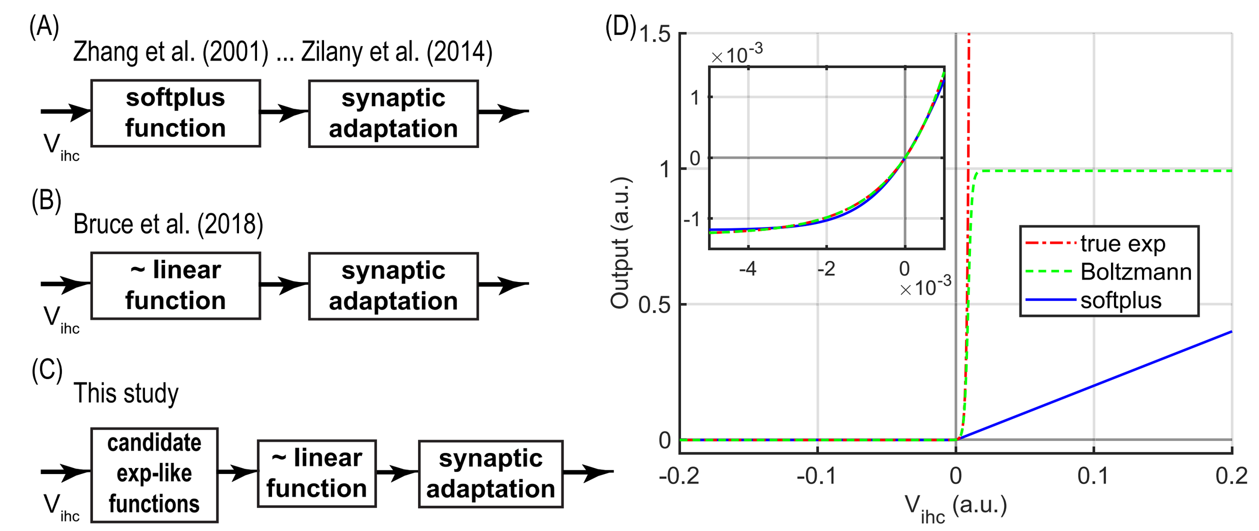

Figure 4: Panels A–C depict the evolution of the IHC to synapse mapping functions used from Zhang et al. (2001) to the present study. The very gradually saturating symmetrical nonlinearity of the Bruce et al. (2018) model is referred to here as being approximately linear. In panel C and the text of the poster, the three candidate functions inserted before the approximately linear function are referred to as "exponential-like" functions. Panel D plots the three candidate functions, the softplus function (Eqn. 1), the true exponential function (Eqn. 2), and the Boltzmann function (Eqn. 3), over the full range of IHC potentials produced by the model. Inset: Zoomed-in plot of the three exponential-like functions for small input values around $V_{ihc} = 0$.

- In the Bruce et al. (2018) model, the lack of exponential-like I/O behavior for sound levels near threshold could lead to an incorrect growth of synchronization and mean rate with sound level.
- The goal of the present study was to determine whether adding a softplus function back into the mapping from the IHC potential to the synaptic drive (Fig. 4C) produces exponential-like I/O behavior near threshold for model ANFs while maintaining correct I/O function and period histogram shapes at higher sound pressure levels. The simulation results using the softplus function were compared to results obtained with: the original mapping function from Bruce et al. (2018), a true exponential function in place of the softplus function, or a Boltzmann function in place of the softplus function (Fig. 4D). We will refer to the softplus function, the true exponential function, and the Boltzmann function collectively as the candidate "exponential-like" functions.

II. METHODS

- In the Bruce et al. (2018) model, an offset value is added after the approximately linear mapping to produce the given spontaneous rate. Therefore, all three candidate exponential-like functions are shifted down so that the output is zero when the input is zero.
- The shifted softplus function (Fig. 4D) is given by:

$$O_{sp}(t) = p_{1sp}\left[\log_e\left(1 + e^{p_{2sp}V_{ihc}(t)}\right) - \log_e 2\right], \tag{1}$$

where $V_{ihc}(t)$ is the IHC potential (in arbitrary units) at time t, p_{1sp} and p_{2sp} are the amplitude and slope parameters, respectively, for the softplus function, and the term $-\log_e 2$ shifts the function down.
- The default slope parameter was set to $p_{2sp} = 1165$, matching the value from Zhang et al. (2001) for low CFs. The existing mapping function from the Bruce et al. (2018) model already sets the fiber threshold, so the slope of the shifted softplus function is set to one at $V_{ihc} = 0$, which is achieved when $p_{1sp} \cdot p_{2sp} = 2$, and thus the default value for p_{1sp} was set to 1.72×10^{-3}.
- The alternative exponential-like functions were a shifted true exponential function:

$$O_{exp}(t) = p_{1exp}\left[e^{p_{2exp}V_{ihc}(t)} - 1\right], \tag{2}$$

and a shifted Boltzmann function:

$$O_{bltz}(t) = \frac{1}{1 + p_{1bltz}\,e^{-p_{2bltz}V_{ihc}(t)}} - \frac{1}{1 + p_{1bltz}}, \tag{3}$$

with their respective amplitude ($p_{1exp/bltz}$) and slope ($p_{2exp/bltz}$) parameters.
- The default parameters for these alternative models were obtained by performing a nonlinear least-squares fit to the default softplus function over the range of input values V_{ihc} between -5×10^{-3} and 1×10^{-3} using the MATLAB Curve Fitting Toolbox, giving the functions plotted in Fig. 4D with parameters $p_{1exp} = 1.268\times10^{-3}$, $p_{2exp} = 747.9$, $p_{1bltz} = 787.77$, and $p_{2bltz} = 749.69$. Because of the very rapid increase in the output of the true exponential function with positive IHC potentials, the maximum output was limited to a value of 30.
- Simulations were run in MATLAB version 2022a under Linux on high-performance computing clusters provided by the Digital Research Alliance of Canada.
- The acoustic stimulation paradigm and data analysis protocols were based on those of Horst et al. (2018), and simulations were run for three low-CF model fibers with CFs and spont rates similar to example low-, medium-, and high-spont fibers from Horst et al. (2018). In summary:
  - Acoustic stimulus inputs to the model were 1-second long pure tones with 5-ms long linear rise and fall times. Model spike trains were generated in response to 400 repetitions of each stimulus, with a 0.5-second silent period between each presentation.
  - Period histograms with 32 bins per stimulus period were computed, excluding spikes in the first and last 10 ms of the stimulus response.
  - To compute instantaneous input/output curves, Horst et al. (2018) found the phase of the fundamental frequency of the period histogram via the discrete Fourier transform and shifted the input waveform to that phase. However, visual comparison of period histograms is more straightforward if they are shifted to be roughly at sine phase (Johnson, 1980). Therefore, instead of shifting the stimulus phase, we have shifted the period histograms to sine phase, using the same method as Horst et al. (2018) to calculate the original phase, before computing the I/O curves.

III. RESULTS

- Figure 5 shows simulation results for high SR model fibers. The original Bruce et al. (2018) model has I/O curves for stimulus levels around threshold in panel A being very close to linear across the three presentation levels (see the red line for a linear fit to the −5 dB SPL case), except for strong positive rectification when the instantaneous input pressure is below −0.025 mPa, because the instantaneous rate cannot go below zero.
- In Fig. 5B, insertion of the softplus function (Eq. 1) with the default parameters leads to some exponential-like deviation from linearity for the −5 and 0 dB SPL cases, and soft rectification is observed for pressures less than −0.02 mPa. (Similar I/O curves are produced by the true exponential and Boltzmann functions, since those functions are very similar to the softplus function for small input values—see the inset of Fig. 4D.)
- Increasing the value of the slope parameter p_{2sp} for the softplus function while maintaining $p_{1sp} \cdot p_{2sp} = 2$ leads to even stronger exponential-like curvature for the I/O functions near threshold (Fig. 5C).
- Consistent with the results of Horst et al. (2018), the slope of the I/O curves for positive input values becomes increasingly shallow for the softplus model as the stimulus level increases from threshold to saturation across the dynamic range of the fiber (Fig. 5D). (This drop in the slope of the I/O curves with increasing sound levels above threshold is also observed in the Bruce et al. (2018) model with the original mapping function.)
- The period histograms for the softplus model with default parameters in Fig. 5E exhibit an increase in the strength of phase locking as the stimulus level is increased above threshold (15 and 30 dB SPL cases) and that is maintained as the level moves into the saturation region of the rate-level curve (60 dB SPL case).

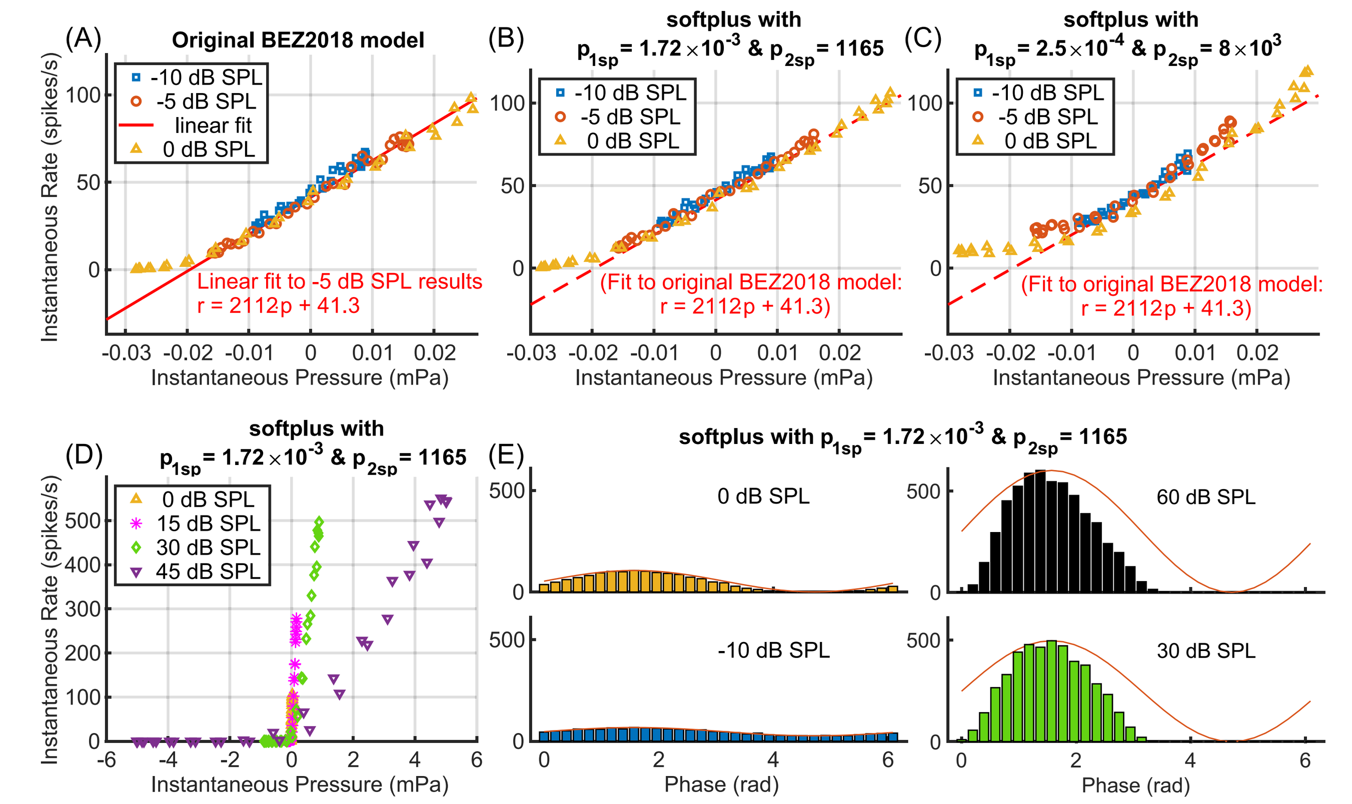

Figure 5: Simulation results for model high-spont fibers with spont rate = 37 spikes/s, CF = 591 Hz, and stimulus frequency = 600 Hz. Panels A–C show input/output curves for stimulus levels around threshold for three different model variations: (A) the original mapping function of Bruce et al. (2018), (B) the softplus function with default parameters, and (C) the softplus function with modified parameters to give increased curvature. A linear fit to the −5 dB SPL I/O curve for the original model is shown on all three plots. Panels D & E show responses for stimulus levels across the dynamic range of the fiber, into the saturation region, for the softplus function with default parameters: (D) input/output curves, and (E) period histograms. The period histograms are all shifted to be at sine phase. One cycle of the stimulus is depicted by the thin red curves, scaled to the maximum and minimum values of each period histogram.

- Figure 6 provides plots of SI versus level (blue curves with labels on the left-side axes) and mean rate versus level (red curves with labels on the right-side axes). In panels A–C, the responses of the softplus model with default parameters are compared to those of the original Bruce et al. (2018) model for example high spont rate (HSR), medium spont rate (MSR), and low spont rate (LSR) fibers. It can be observed that the softplus model leads to a small but significant boost in synchronization to pure-tone stimuli over the range of 0 to 20 dB SPL in all three fiber types. The softplus function also leads to a more substantial increase in the growth of the mean rate with increasing level for all three model fiber types over their entire dynamic range.
- Panels D and E of Fig. 6 show SI-level and rate-level plots for the three spont types for the variants of the model with the true exponential function and the Boltzmann functions, respectively. Both of these model variants exhibit too sharp a growth in the SI-level and rate-level curves above threshold, with the SI-level curve then dipping dramatically above 25 dB SPL and the rate-level curves saturating in an unrealistic fashion.
- Observation of example period histograms for the true exponential variant of the model plotted in Fig. 6F shows that the dip in SI values is due to the model fiber being driven abnormally hard at the onset of each positive stimulus cycle, such that synaptic adaptation and ANF refractoriness produce a steep drop to a fairly constant firing rate for the remainder of the positive cycle. The saturation of the Boltzmann function, compared to the continued growth of the true exponential function, leads to that model variant not driving the synapse quite so hard, so the drop in synchronization is not as pronounced, but it is still inconsistent with the physiological data.

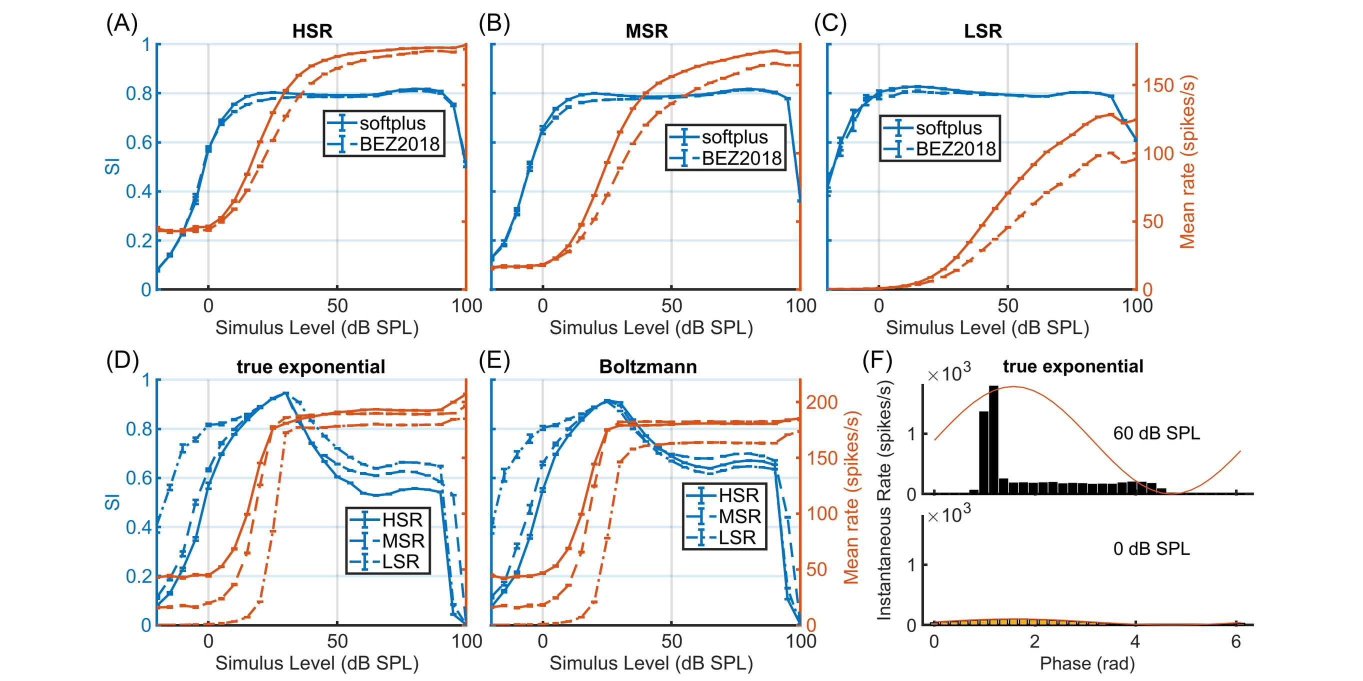

Figure 6: Panels A–C show plots of the synchronization index (SI; blue curves) and mean rate (red curves) versus level for two model variations, the original mapping function of Bruce et al. (2018) and the softplus function with default parameters, for three different model fibers types: (A) high spont rate (HSR) fibers with spont rate = 37 spikes/s, CF = 591 Hz, and stimulus frequency *F*0 = 600 Hz; (B) medium spont rate (MSR) fibers with spont rate = 12 spikes/s, CF = 700 Hz, and *F*0 = 700 Hz; (C) low spont rate (LSR) fibers with spont rate = 0.1 spikes/s, CF = 550 Hz, and *F*0 = 550 Hz. Panels D & E show SI-level and rate-level curves for example HSR, MSR, and LSR fibers for two model variations for the exponential-like function, (D) the true exponential function and (E) the Boltzmann function (see Fig. 4D). SI-level and rate-level curves are the mean of 10 simulations, with error bars showing the s.e.m. (F) Period histograms for a model HSR fiber with the true exponential function for two different sound levels, one near threshold and the other in the saturation region of the rate-level curve.

IV. DISCUSSION AND CONCLUSIONS

- The results of this study show that a softplus function used in the mapping from IHC potential to synaptic drive better explains instantaneous I/O curves, period histograms, and SI-level and rate-level curves of cat ANFs than does a true exponential or Boltzmann function when inserted into the model of Bruce et al. (2018).
- This differs from the results of Peterson and Heil (2020, 2021) because the Boltzmann function in their model exhibits hard saturation, such that the inputs to their exponential function extend over a restricted range of values, and the output of their exponential function therefore never grows unreasonably large (see Fig. 2).
- Quantitative comparison with a large ANF dataset, such as that of Peterson and Heil (2020, 2021), is needed to determine: i) whether the softplus function should remain before the approximately linear mapping function or be moved to after it, and ii) optimal parametrization of the softplus and mapping function.

Model code available to download via the link
`https://www.ece.mcmaster.ca/~ibruce/zbcANmodel/zbcANmodel.htm`
or the QR code to the right.

REFERENCES

Bruce, I. C., Erfani, Y., and Zilany, M. S. A. (2018). A phenomenological model of the synapse between the inner hair cell and auditory nerve: Implications of limited neurotransmitter release sites. *Hearing Research*, 360:40–54.

Cheatham, M. A. and Dallos, P. (2000). The dynamic range of inner hair cell and organ of corti responses. *The Journal of the Acoustical Society of America*, 107(3):1508–1520.

Dugas, C., Bengio, Y., Bélisle, F., Nadeau, C., and Garcia, R. (2000). Incorporating second-order functional knowledge for better option pricing. In Leen, T., Dietterich, T., and Tresp, V., editors, *Advances in Neural Information Processing Systems*, volume 13. MIT Press.

Horst, J. W., McGee, J., and Walsh, E. J. (2018). Input-output curves of low and high spontaneous rate auditory nerve fibers are exponential near threshold. *Hearing Research*, 367:195–206.

Johnson, D. H. (1980). The relationship between spike rate and synchrony in responses of auditory-nerve fibers to single tones. *The Journal of the Acoustical Society of America*, 68(4):1115–1122.

Osses Vecchi, A., Varnet, L., Carney, L. H., Dau, T., Bruce, I. C., Verhulst, S., and Majdak, P. (2022). A comparative study of eight human auditory models of monaural processing. *Acta Acustica*, 6:17.

Peterson, A. J. and Heil, P. (2020). Phase locking of auditory nerve fibers: The role of lowpass filtering by hair cells. *The Journal of Neuroscience*, 40(24):4700–4714.

Peterson, A. J. and Heil, P. (2021). A simplified physiological model of rate-level functions of auditory-nerve fibers. *Hearing Research*, 406:108258.

Zhang, X., Heinz, M. G., Bruce, I. C., and Carney, L. H. (2001). A phenomenological model for the responses of auditory-nerve fibers: I. Nonlinear tuning with compression and suppression. *The Journal of the Acoustical Society of America*, 109(2):648–670.

Zilany, M. S. A., Bruce, I. C., and Carney, L. H. (2014). Updated parameters and expanded simulation options for a model of the auditory periphery. *The Journal of the Acoustical Society of America*, 135(1):283–286.

Zilany, M. S. A., Bruce, I. C., Nelson, P. C., and Carney, L. H. (2009). A phenomenological model of the synapse between the inner hair cell and auditory nerve: Long-term adaptation with power-law dynamics. *The Journal of the Acoustical Society of America*, 126(5):2390–2412.

brucei@mcmaster.ca | abigail.buller@mail.mcgill.ca | muhammad.zilany@qatar.tamu.edu

This research was funded by NSERC Discovery Grant #RGPIN-2018-05778 (ICB) and was enabled in part by support provided by Compute Ontario (www.computeontario.ca) and the Digital Research Alliance of Canada (www.alliancecan.ca).